J. Electrochem. Sci. Eng. **00(0)** (2022) 000-000; http://dx.doi.org/10.5599/jese.1153

Open Access : : ISSN 1847-9286

www.jESE-online.org

Original scientific paper

A sensitive voltammetric sensor for specific recognition of vitamin C in human plasma based on $MAPbI_3$ perovskite nanorods

Gizem Tiris[1], Yasamin Khoshnavaz[2], Elif Naz Öven[2], Mohammad Mehmandoust[2,3,✉] and Nevin Erk[2,3,✉]

[1]*Bezmialem Vakif University, Faculty of Pharmacy, Department of Analytical Chemistry, 34093 İstanbul, Turkey*

[2]*Ankara University, Faculty of Pharmacy, Department of Analytical Chemistry, 06560 Ankara, Turkey*

[3]*Sakarya University, Biomaterials, Energy, Photocatalysis, Enzyme Technology, Nano & Advanced Materials, Additive Manufacturing, Environmental Applications, and Sustainability Research & Development Group (BIOENAMS R&D Group), 54187 Sakarya, Turkey*

Corresponding authors: ✉mehmandoust@ankara.edu.tr; ✉erk@pharmacy.ankara.edu.tr; *Tel.: +90-5526828057*

Received: October 31, 2021; Accepted: January 19, 2021; Published: January 28, 2022

Abstract

A novel and sensitive electrode was suggested for the rapid determination of ascorbic acid (AA) using a glassy carbon electrode (GCE) modified with synthesized $MAPbI_3$ and L-cys (L-cys/$MAPbI_3$/GCE). Determination of ascorbic acid as an important component of the human diet due to help in decreasing blood pressure and improving endothelial function is crucial. The synthesized $MAPbI_3$ was characterized by different methods, including transmission electron microscopy (TEM), scanning electron microscopy (SEM), energy-dispersive X-ray spectroscopy (EDX), and X-ray diffraction (XRD). The fabricated electrode exhibited superior electrical conductivity and fast electron transfer kinetics. The results illustrated that the developed electrode had an outstanding electrocatalytic activity towards the oxidation of AA in 0.1 M Britton–Robinson buffer(B-R) as a supporting electrolyte. The modified electrode demonstrated a linear range in differential pulse voltammetry of 0.02–11.4 μM with a low detection limit of 8.0 nM for ascorbic acid. It can be stated that the proposed sensor can be successfully applied to the determination of ascorbic acid in human plasma samples.

Keywords

Voltammetry, ascorbic acid, $MAPbI_3$, cysteine, human plasma

Introduction

Ascorbic acid (AA), namely vitamin-C, is a six-carbon lactone produced by plants and some animal species but not by humans or other primates, and it must be obtained from food. Vitamin C's biological action is critical for the skin's proper functioning. L-ascorbic acid is the more physiologically active of the two forms of vitamin C found in nature in fruits and vegetables such as oranges, broccoli, leafy greens, grapefruit, and peppers, and is the more useful, but the "D" form can be made via chemical synthesis but has no significant biological role. L-ascorbic acid protects against hydroxyl radicals, superoxide, and singlet oxygen, among other things. Furthermore, it lowers the membrane-bound antioxidant -tocopherol. Diabetes, coronary artery disease, hypertension, and chronic heart failure benefit from L-ascorbic acid's endothelium-dependent vasodilation. Monitoring AA content should be regarded as an essential and relevant task for evaluating the quality of final food items, raw materials, and various other substances, considering the nutritional value and therapeutic AA characteristics.

Although a variety of analytical methods are utilized to determine AA, including spectroscopic [1], chromatographic[2,3], the electrochemical methods have been widely performed in recent years [4-8] because of their rapid response, high sensitivity, good stability, superior selectivity, and cost-effectiveness [9-11]. However, enhancing electrochemical performance in real samples necessitates the development of well-defined chemical structures and porous nanomaterials [12-14]. Recently, there is a big jump in fine-tuning the properties of nanomaterials and utilizing them in various applications [15-17]. In terms of materials, methylammonium lead iodide ($CH_3NH_3PbI_3$ or $MAPbI_3$), a perovskite-like organic-inorganic metal halide, has emerged as a viable low-cost material for next-generation high-efficiency perovskite solar cells[18]. Furthermore, the sensitivity of perovskite materials allows this disadvantage to be turned into an advantage [19]. As far as we know, this is the first sensor system using $MAPbI_3$ as a modifier that has appropriate results for measuring one of the main parts of the human diet. In biological systems, cysteine, a thiol-containing non-essential amino acid, plays a significant function. It's found in a lot of proteins and acts as a precursor for protein synthesis, and is also utilized as a modifier in the production of electrochemical sensors. In electrochemical investigations, cysteine and cysteine-containing materials adorned electrodes are particularly popular. In this study, L-cys were modified on $MAPbI_3$, and the resulting nanomaterial was utilized to modify the GCE surface to fabricate the sensor. A voltammetric method was developed using L-cys@$MAPbI_3$/GCE and utilized to determine AA in the human plasma samples. Furthermore, our study exhibits a sensitive and selective sensor for AA determination with a LOD value of 8.0 nM in a wider linear range of 0.02 to 11.4 µM. Finally, the sensor's applicability is demonstrated by its application to human plasma, which yielded satisfactory recovery results.

Experimental

Materials:

Methylammonium iodide, lead iodide, oleic acid, oleylamine, L-cysteine were acquired from Sigma Aldrich Co. (Germany). A human plasma sample was also obtained from Sera-Flex Inc (Turkey). All chemicals were of analytical grade.

Apparatus

XRD patterns were collected by Rigaku Smart Lab XRD. Scanning electron microscopy images and energy-dispersive X-ray spectroscopy were recorded by ZEISS Gemini at 3.00 kV. Electrochemical methods such as cyclic voltammetry (CV), differential pulse voltammetry (DPV), and electrochemical

(cc) BY

impedance spectroscopy (EIS) were carried out through PGSTAT128N (Metrohm Inc., Switzerland). TEM images were obtained using an FEI Tecnai G2 Spirit microscope (Oregon, USA) at 120 kV.

The synthesis procedure of $MAPbI_3$

$MAPbI_3$ nanorods were synthesized using a facile ligand-assisted deposition approach. To begin with, 16.0 mg methylammonium iodide and 40.0 mmol lead iodide were dissolved in 2.0 mL dimethylformamide (DMF) and stirred for 24 h. Following, 400.0 µL oleic acid and 50.0 µL oleylamine were introduced into the resultant dispersion and kept stirring for 4 h. Moreover, 200.0 µL of the mixture solution was poured into 5.0 mL chloroform solution, stirring at the dark conditions over 5.0 h to obtain a dark brownish solution as $MAPbI_3$ nanorods were obtained [20].

Preparation of fabricated electrode

Before modification, the bare electrode was polished with aluminum slurries (1.0 and 0.05 µm) and then washed by using HNO_3 (10 vol.%), ethanol, and distilled water, respectively. Afterward, 8.0 µL of $MAPbI_3$ was dropped onto the GCE and allowed to dry at room temperature. In the following, 5.0 µL of L-cys solution (2.0 mg mL^{-1}) was dropped on the $MAPbI_3$ electrode surface and was left to dry at room temperature [21].

Preparation of real sample

For the preparation procedure for the human plasma as the real sample, firstly, 1.0 mL of human plasma was treated with 1.0 mL of acetonitrile to eliminate the proteins. After that, the solution was centrifuged over 20 minutes at 10 °C at 6000 rpm. Before being put into the electrochemical cell, the samples were diluted to a certain concentration using B-R buffer at pH 7.0. [14].

Results and discussion

Characterization

Figure 1 illustrates the X-ray diffraction patterns recorded in the 2θ ranging from 5.0 to 90.0° for $MAPbI_3$. The typical peaks at 19.40, 24.47, 29.42 and 30.89° corresponded to (110), (202), (004), (220) lattice planes of the tetragonal phase perovskite, respectively [22-24]. Moreover, as shown in Fig. 1, the XRD pattern of the $MAPbI_3$ presents all characteristic peaks of $MAPbI_3$ with good tetragonal structures with good crystallinity [25,26].

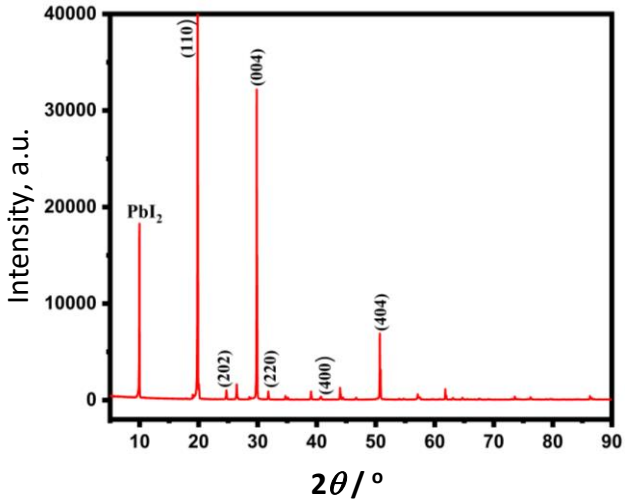


Figure 1. *XRD pattern of $MAPbI_3$*

SEM and TEM images of pristine $MAPbI_3$ are displayed in Figure 2. As shown in Figures 2A and 2B, the pristine $MAPbI_3$ nanorods have a size of 50.0-200.0 nm, relatively smooth surfaces, and high crystallinity. SEM image (Figure 2C) indicates the formation of highly crystalline, dense, and pinhole-free $MAPbI_3$. Elemental composition and percentage of as-synthesized $MAPbI_3$ were validated through EDX analysis(Figure 2D). It was clearly observed sharp peaks relative to Pb, N, and I.

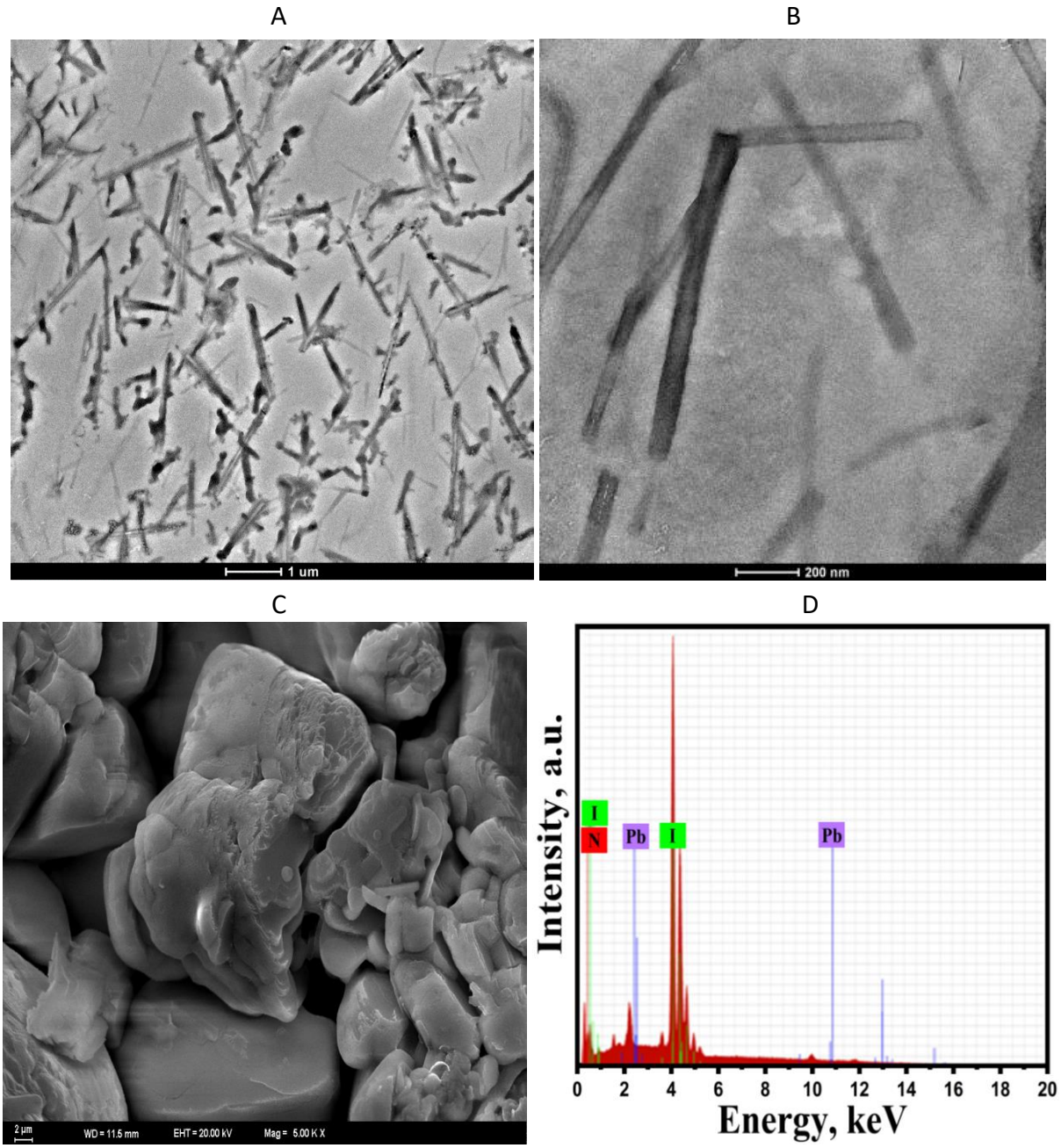


Figure 2. *A and B - TEM and C - SEM images of $MAPbI_3$; D - EDX spectrum of $MAPbI_3$*

Electrochemical characterization of the L-cys@$MAPbI_3$/GCE:

The effect of the modification of electrode surface was studied via DPV techniques. Figure 3 showed the DPV response of the bare electrode, $MAPbI_3$/GCE, and L-cys@$MAPbI_3$/GCE to a fixed concentration of AA (0.5 µM). Obviously, it can be seen that the presence of the $MAPbI_3$ and L-cys increased the signal magnitude of the glassy carbon-based electrode to determine AA. In other words, such a described behavior can be related to the electrocatalytic activity of L-cys@$MAPbI_3$/GCE for electro-oxidation of AA.

(cc) BY

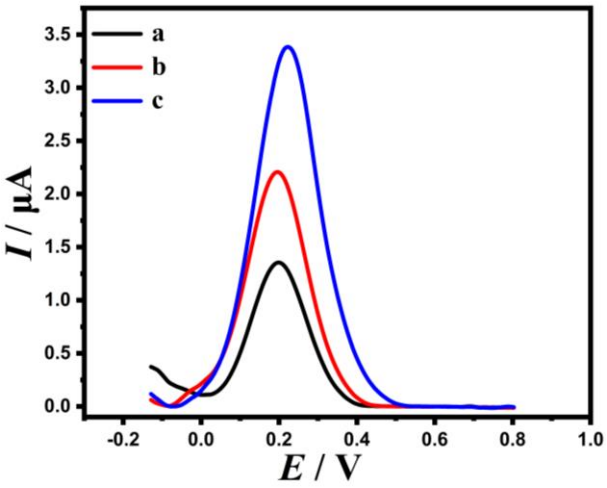


Figure 3. *DPVs of bare electrode (a), $MAPbI_3$/GCE (b), L-cys/$MAPbI_3$/GCE in 0.1 M B-R buffer at pH 7.0 containing 0.5 µM AA.*

According to the obtained voltammograms in Figure 4A, L-cys@$MAPbI_3$/GCE illustrated the highest electrochemical activity compared to the bare electrode (5.63 to 10.2 µA). In addition, the values of ΔE_p were calculated as 107.4 mV for L-cys@$MAPbI_3$/GCE and 298.3 mV for bare electrode, indicating the synergic effect between L-cys and $MAPbI_3$.

EIS experiments were also performed to extract impedance characteristics of the fabricated electrode in 0.1 M KCl containing 5.0 mM [$Fe(CN)_6^{-3/-4}$] solution as a redox probe. The Nyquist plots of the obtained data are shown in Figure 4B. The charge transfer resistance magnitude at the respective electrodes was ascribed to the diameters of the depressed semicircles. As shown, the charge transfer resistance at L-cys@$MAPbI_3$/GCE surface is decreased about 1.7-fold compared to the bare electrode (23.57 kΩ), indicating fast electron transfer on the electrode surface [27]. Results confirmed that the presence of L-cys and $MAPbI_3$ increases the electrode surface's conductivity [28].

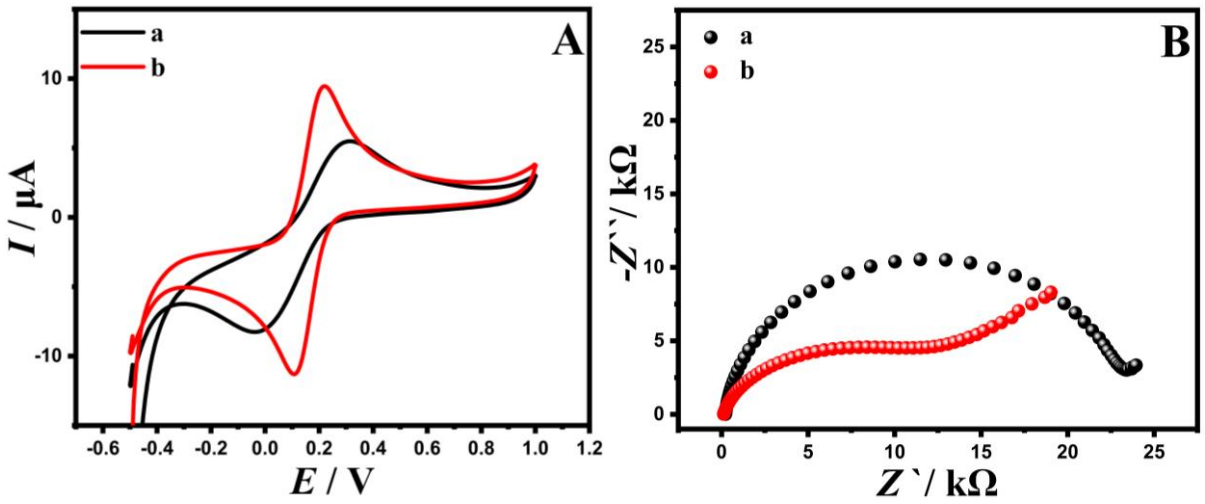


Figure 4. *(A); CVs and (B); EIS of bare (a) and L-cys@$MAPbI_3$/GCE (b) in in 0.1 M KCl containing 5.0 mM [$Fe(CN)_6^{-3/-4}$].*

pH and CV studies

The effect of pH on the oxidation of 1.0 µM AA was depicted in Figure 5A. The pH value of the B-R buffer was adjusted using 0.1 M HCl and NaOH. The oxidation currents of AA were observed in the pH range between 2.0 to 8.0 in 0.1 M B-R buffer. The peak current enhanced when the pH

increased until pH 7.0, and after pH 7.0, the peak current decreased with a further increase of pH. Finally, pH 7 was selected for further experiments.

The diffusion-controlled mechanism at L-cys@$MAPbI_3$/GCE was investigated using the linear relationship between the square root of the scan rates and current peak at different scan rates (10.0 to 400.0 mV s^{-1}). The oxidation peak changed to positive potentials with increasing scan rates, as seen in Figure 5B. As shown in Figure 5C, the anodic peak currents enhanced linearly with the square root of scan rate, indicating that the redox reaction of the electrodes was a diffusion-controlled process [29]. Therefore, the electrocatalytic behavior of the electrode was improved. As for an irreversible electrochemical reaction, the E_{pa} is determined by the following (Eq. 1):

$$E_{pa} = E^0 - \frac{RT}{\alpha nF}\ln\left(\frac{\alpha nF}{RTK}\right) - \left(\frac{RT}{\alpha nF}\right)\ln\nu \quad (1)$$

According to the linear relationship of E_{pa} against ln ν (Figure 5D), the value of *n* was observed to be approximately 1.0.

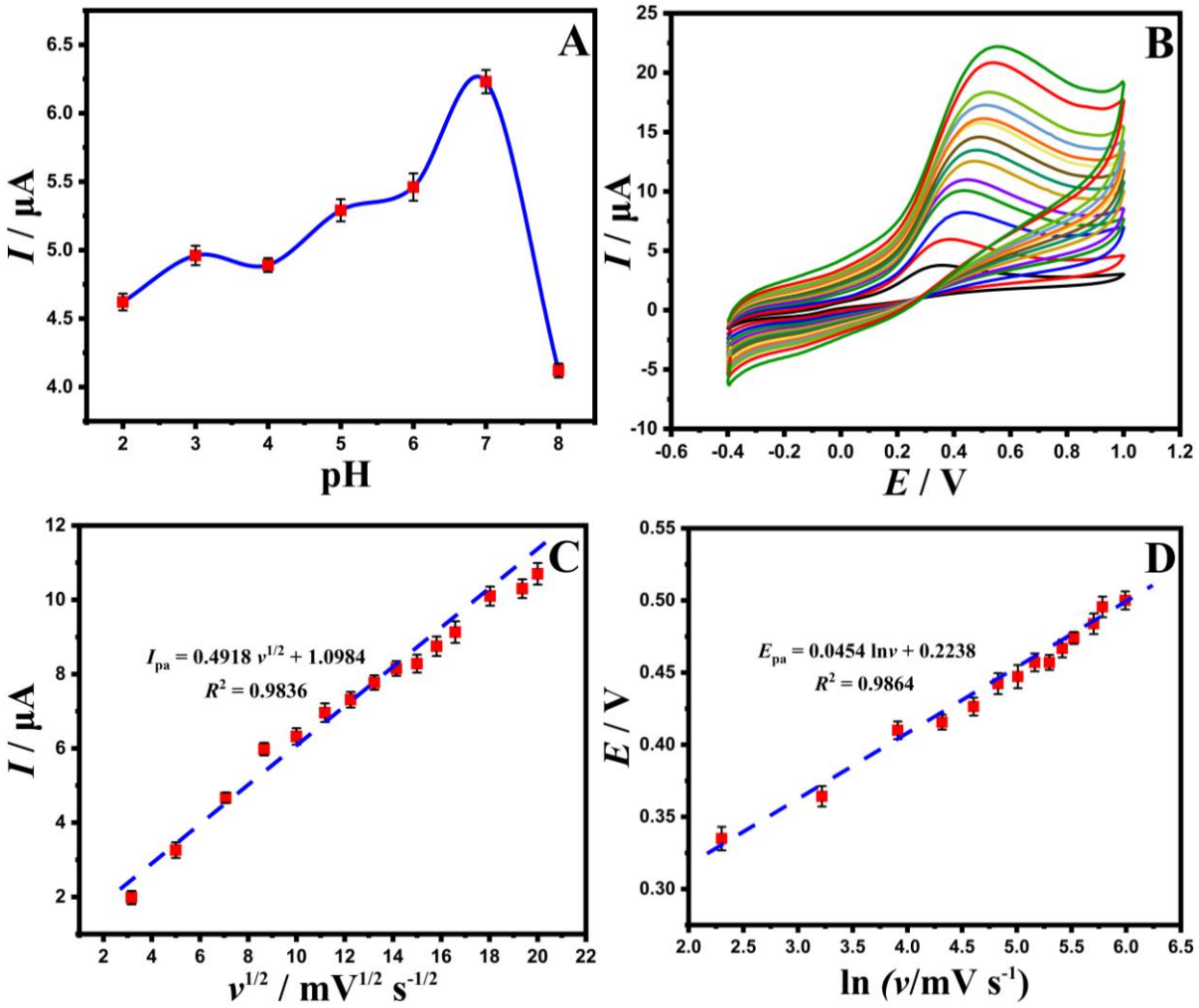


Figure 5. *A - The I_{pa} vs. pH curve for electro-oxidation of AA at the surface of L-cys@$MAPbI_3$/GCE; B - CVs of L-cys@$MAPbI_3$/GCE in the presence of 0.1 M KCl containing 1.0 µM AA; C - The plot of I_{pa} against $\nu^{1/2}$ relative to electro-oxidation of 1.0 µM AA at L-cys@$MAPbI_3$/GCE; D - The plot of E_{pa} vs. natural logarithm*

Chronoamperometry study

The chronoamperometric study was conducted using a developed electrode at 0.6 V in the presence of different concentrations of ascorbic acid (50.0 and 100 µM) in 0.1 B-R buffer (pH 7.0).

(cc) BY

By plotting *I* versus $t^{-1/2}$ and Cottrell's equation (Figure 6), the diffusion coefficient (*D*) was estimated as 8.99×10^{-7} cm^2 s^{-1}.

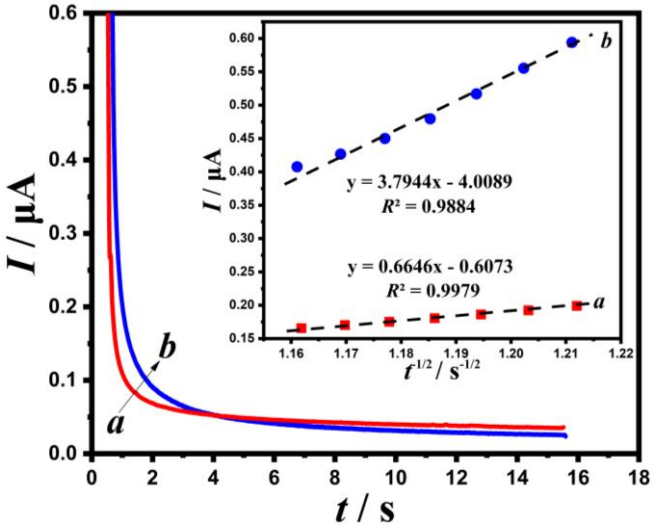


Figure 6. *Chronoamperograms obtained at L-cys@MAPbI₃/GCE, (Inset) Cottrell's plot for the data from the chronoamperograms*

Determination of ascorbic acid

Figure 7A demonstrated the DPV curves of various ascorbic acid concentrations at the L-cys@MAPbI$_3$/GCE in 0.1 M B-R at pH 7.0. The increase in the current values was linearly related to the AA concentration in the concentration range of 0.02 to 11.4 µM (Figure 7B). The limit of detection (LOD) was 8.0 nM AA, according to the definition of LOD = 3*sb*/*m* [30]. cys@MAPbI$_3$/GCE has a lower detection limit for AA compared with other modified electrodes (Table 1).

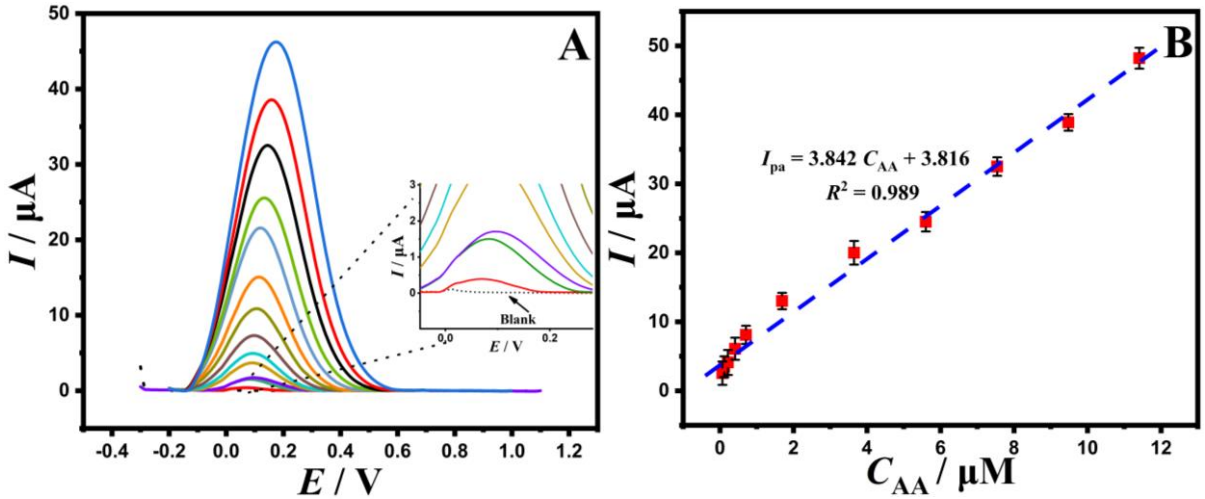


Figure 7. *A - DPVs of L-cys@MAPbI₃/GCE with increasing AA concentration; B - The plot of the oxidation current as a function of AA concentration*

Table. 1. *Comparison of different sensors for the determination of AA*

Method	Modified	Linear range, µM	LOD, µM	Ref.
DPV	CL-TiN/GCE	50-1500	1.50	[31]
Amperometry	GCHs-CNPTs/GCE	10-3570	1.09	[32]
Amperometry	TOAB/YD/MWCNT/GCE	0.0187–1.85	0.18	[33]
Amperometry	TOAB/ERGO@YD/GCE	1.33-1460	0.28	[34]
DPV	L-cys@MAPbI$_3$/GCE	0.02-11.4	0.008	This work

Reproducibility, repeatability

The reproducibility, repeatability, and selectivity of L-cys@$MAPbI_3$/GCE were investigated by recording DPV of 1.0 µM AA at pH 7.0. The relative standard deviations (RSD) of 2.3 and 1.2 % for five successive recorded signals (repeatability) and five independents (reproducibility) of L-cys@$MAPbI_3$/GCE, respectively that confirmed outstanding repeatability and reproducibility for L-cys@$MAPbI_3$/GCE as an electroanalytical sensor toward AA.

Determination of ascorbic acid in the human plasma sample

The utilization of the developed sensor L-cys@$MAPbI_3$/GCE in the real sample was also observed using the standard addition method in human plasma samples. The recovery of the spiked samples was obtained from 97.5 to 102.8 %. Results show that the developed electrochemical sensor will be useful for diagnosing biological samples.

Conclusions

In summary, a sensor based on L-cys@$MAPbI_3$ was fabricated on a glassy carbon electrode to determine ascorbic acid. The results offered a well-defined oxidation peak for oxidation of ascorbic at L-cys@$MAPbI_3$/GCE, which were large enough to determine AA. Moreover, the fabricated L-cys@$MAPbI_3$/GCE exhibited acceptable results as a working electrode with a low detection limit, appropriate reproducibility, and repeatability. The fabricated sensor was successfully utilized to analyze AA in the real sample. The as-fabricated electrode could be an outstanding candidate as an alternative analytical approach for determining the trace amount of AA in clinical samples.

***Acknowledgments**: This work was supported by the Scientific Research Projects Commission of Ankara University (Project Number: 21B0237005 and 21H0237005).*

References

[1] J. Wang, X. Peng, D. Li, X. Jiang, Z. Pan, A. Chen, L. Huang, J. Hu, *Microchimica Acta* **185** (2018) 42. https://doi.org/10.1007/s00604-017-2557-9

[2] E. Kishida, Y. Nishimoto, S. Kojo, *Analytical Chemistry* **64** (1992) 1505-1507. https://doi.org/10.1021/ac00037a035

[3] N. Ismillayli, D. Hermanto, I. S. Andayani, R. Honiar, U. K. Zuryati, B. Mariana, L. M. Shofiyana, *Al-Kimia* **8** (2020) 168-176. http://journal.uin-alauddin.ac.id/index.php/al-kimia/article/view/15097

[4] A. A. Ensafi, H. Karimi-Maleh, *International Journal of Electrochemical Science* **5** (2010) 392-406. http://electrochemsci.org/papers/vol5/5030392.pdf

[5] H. Karimi-Maleh, M. Hatami, R. Moradi, M. A. Khalilzadeh, S. Amiri, H. Sadeghifar, *Microchim Acta* **183** (2016) 2957-2964. https://doi.org/10.1007/s00604-016-1946-9

[6] H. Karimi-Maleh, F. Karimi, L. Fu, A. L. Sanati, M. Alizadeh, C. Karaman, Y. Orooji, *Journal of Hazardous Materials* **423** (2022) 127058. https://doi.org/10.1016/j.jhazmat.2021.127058

[7] H. Karimi-Maleh, F. Tahernejad-Javazmi, M. Daryanavard, H. Hadadzadeh, A. A. Ensafi, M. Abbasghorbani, *Electroanalysis* **26** (2014) 962-970. https://doi.org/10.1002/elan.201400013

[8] H. Karimi-Maleh, A. A. Ensafi, H. R. Ensafi, *Journal of the Brazilian Chemical Society* **20** (2009) 880-887. https://pdfs.semanticscholar.org/58af/6c3217147877cf86331e506d81147793dc60.pdf

[9] M. Mehmandoust, F. Uzcan, M. Soylak, N. Erk, *Chemosphere* (2021) 132809. https://doi.org/10.1016/j.chemosphere.2021.132809

[10] M. Mehmandoust, N. Erk, C. Karaman, O. Karaman, *Chemosphere* (2021) 132807. https://doi.org/10.1016/j.chemosphere.2021.132807

[11] J. Mohanraj, D. Durgalakshmi, R. A. Rakkesh, S. Balakumar, S. Rajendran, H. Karimi-Maleh, *Journal of Colloid and Interface Science* **566** (2020) 463-472. https://doi.org/10.1016/j.jcis.2020.01.089

[12] A. Taherkhani, T. Jamali, H. Hadadzadeh, H. Karimi-Maleh, H. Beitollahi, M. Taghavi, F. Karimi, *Ionics* **20** (2014) 421-429. https://doi.org/10.1007/s11581-013-0992-0

(cc) BY

[13] J. B. Raoof, R. Ojani, H. Karimi-Maleh, *Journal of Applied Electrochemistry* **39** (2009) 1169-1175. https://doi.org/10.1007/s10800-009-9781-x
[14] M. Mehmandoust, N. Erk, C. Karaman, F. Karimi, S. Salmanpour, *Micromachines* **12** (2021) 1334. https://doi.org/10.3390/mi12111334
[15] A. A. Ensafi, S. Dadkhah-Tehrani, H. Karimi-Maleh, *Analytical Sciences* **27** (2011) 409-414. ttps://doi.org/10.2116/analsci.27.409
[16] E. Mirmomtaz, A.A. Ensafi, H. Karimi-Maleh, *Electroanalysis* **20** (2008) 1973-1979. https://doi.org/10.1002/elan.200804273
[17] H. Karimi-Maleh, A. Khataee, F. Karimi, M. Baghayeri, L. Fu, J. Rouhi, C. Karaman, O. Karaman, R. Boukherroub, *Chemosphere* (2021) 132928. https://doi.org/10.1016/j.chemosphere.2021.132928
[18] A. D. Sheikh, V. Vhanalakar, A. Katware, K. Pawar, P.S. Patil, *Advanced Materials Technologies* **4** (2019) 1900251. https://doi.org/10.1002/admt.201900251
[19] Q. Wang, S. Yu, M. Ma, X. Wu, W. Qin, *Materials Today Chemistry* **12** (2019) 343-352. https://doi.org/10.1016/j.mtchem.2019.03.007
[20] T. Wang, S. Hou, H. Zhang, Y. Yang, W. Xu, T. Ao, M. Kang, G. Pan, Y. Mao, J*ournal of Alloys and Compounds* **872** (2021) 159589. https://doi.org/10.1016/j.jallcom.2021.159589
[21] M. Mehmandoust, S. Çakar, M. Özacar, S. Salmanpour, N. Erk, *Topics in Catalysis* (2021) 1-13. https://doi.org/10.1007/s11244-021-01479-0
[22] X. Guo, C. McCleese, C. Kolodziej, A. C. Samia, Y. Zhao, C. Burda, *Dalton Transactions* **45** (2016) 3806-3813. https://doi.org/10.1039/C5DT04420K
[23] W. Kong, Z. Ye, Z. Qi, B. Zhang, M. Wang, A. Rahimi-Iman, H. Wu, *Physical Chemistry Chemical Physics* **17** (2015) 16405-16411. https://doi.org/10.1039/C5CP02605A
[24] A. Mishra, Z. Ahmad, F. Touati, R. Shakoor, M. K. Nazeeruddin, *RSC Advances* **9** (2019) 11589-11594. https://doi.org/10.1039/C9RA00200F
[25] J. F. Wang, L. Zhu, B. G. Zhao, Y. L. Zhao, J. Song, X. Q. Gu, Y. H. Qiang, *Scientific Reports* **7** (2017). https://doi.org/10.1038/s41598-017-14920-w
[26] T. I. Alanazi, O. S. Game, J. A. Smith, R. C. Kilbride, C. Greenland, R. Jayaprakash, K. Georgiou, N. J. Terrill, D. G. Lidzey, *RSC Advance* **10** (2020) 40341-40350. https://doi.org/10.1039/D0RA07107B
[27] M. Mehmandoust, N. Erk, M. Alizadeh, S. Salmanpour, *Journal of Food Measurement and Characterization* **15** (2021) 5288-5295. https://doi.org/10.1007/s11694-021-01100-8
[28] M. Mehmandoust, N. Erk, M. Alizadeh, S. Salmanpour, *Journal of Food Measurement and Characterization* (2021) 1-8. https://doi.org/10.1007/s11694-021-01100-8
[29] M. Alizadeh, M. Mehmandoust, O. Nodrat, S. Salmanpour, N. Erk, J*ournal of Food Measurement and Characterization* (2021) 1-8. https://doi.org/10.1007/s11694-021-01128-w
[30] M. Baghayeri, M. Nodehi, H. Veisi, M. B. Tehrani, B. Maleki, M. Mehmandost, *DARU Journal of Pharmaceutical Sciences* **27** (2019) 593-603. https://doi.org/10.1007/s40199-019-00287-y
[31] L. Zhang, J. Feng, K.-C. Chou, L. Su, X. Hou, *Journal of Electroanalytical Chemistry* **803** (2017) 11-18. https://doi.org/10.1016/j.jelechem.2017.09.006
[32] X. Li, Y. Wang, J. Liu, M. Sun, X. Bo, H.-L. Wang, M. Zhou, *Electrochemistry Communications* **82** (2017) 139-144. https://doi.org/10.1016/j.elecom.2017.08.007
[33] D. Huang, X. Li, M. Chen, F. Chen, Z. Wan, R. Rui, R. Wang, S. Fan, H. Wu, *Journal of Electroanalytical Chemistry* **841** (2019) 101-106. https://doi.org/10.1016/j.jelechem.2019.04.041
[34] H. Wu, X. Li, M. Chen, C. Wang, T. Wei, H. Zhang, S. Fan, *Electrochimica Acta* **259** (2018) 355-364. https://doi.org/10.1016/j.electacta.2017.10.122

©2022 by the authors; licensee IAPC, Zagreb, Croatia. This article is an open-access article distributed under the terms and conditions of the Creative Commons Attribution license (https://creativecommons.org/licenses/by/4.0/)